Front. Optoelectron. 2012, 5(1): 112–116
DOI 10.1007/s12200-012-0193-x

RESEARCH ARTICLE

MBE growth of tensile-strained Ge quantum wells and quantum dots

Yijie HUO (✉)[1], Hai LIN[2], Robert CHEN[1], Yiwen RONG[1], Theodore I. KAMINS[1], James S. HARRIS[1]

1 Department of Electrical Engineering, Stanford University, Stanford, California 94305, USA
2 Department of Materials Science and Engineering, Stanford University, Stanford, California 94305, USA

© Higher Education Press and Springer-Verlag Berlin Heidelberg 2012

Abstract Germanium (Ge) has gained much interest due to the potential of becoming a direct band gap material and an efficient light source for the future complementary metal-oxide-semiconductor (CMOS) compatible photonic integrated circuits. In this paper, highly biaxial tensile strained Ge quantum wells (QWs) and quantum dots (QDs) grown by molecular beam epitaxy are presented. Through relaxed step-graded InGaAs buffer layers with a larger lattice constant, up to 2.3% tensile-strained Ge QWs as well as up to 2.46% tensile-strained Ge QDs are obtained. Characterizations show the good material quality as well as low threading dislocation density. A strong increase of photoluminescence (PL) with highly tensile strained Ge layers at low temperature suggests the existence of a direct band gap semiconductor.

Keywords Si photonics, germanium (Ge), tensile strained, photoluminescence (PL)

1 Introduction

Tensile strained germanium (Ge) has attracted much attention recently. It has been reported to have high electron and hole mobility, and theoretical work shows that with about 1.75% biaxial tensile strain, Ge becomes a direct bandgap material [1,2]. Several groups have made strained Ge in several ways: 0.3% tensile strain has been achieved by growing Ge on Si using the thermal expansion coefficient difference between Si and Ge [3]; bulk Ge was strained by mechanical bending [4]; epitaxial Ge was grown on larger lattice constants buffers, such as GeSn or InGaAs [2,5]; and strained Ge quantum dots (QDs) were obtained by mechanical grinding method [6]. In this paper, we report the growths of highly tensile strained Ge quantum wells (QWs) and Ge QDs on InGaAs buffer layers. The changes of Ge material properties under different strain are discussed using transmission electron microscopy (TEM), X-ray diffraction (XRD) and Raman spectroscopy as well as the photoluminescence (PL) phenomenon.

Received September 16, 2011; accepted November 7, 2011

E-mail: yijiehuo@gmail.com

2 Sample preparations

All samples were grown on GaAs(100) wafers in a two-chamber Varian Gen II molecular beam epitaxy (MBE) system with a base pressure of 2×10^{-10} Torr. First step-graded $In_xGa_{1-x}As$ buffer layers were grown in a group III-V chamber. The highest In content in each buffer layers ranges from $x = 0.1$ to $x = 0.4$. Details about the growth recipe can be found elsewhere [7]. The samples were then transferred under ultra high vacuum (1×10^{-9} Torr) to a group IV MBE chamber for Ge growth. A pyrolytic boron nitride effusion cell was used to evaporate 99.9999% pure Ge. For the Ge QW structure, a 10 nm Ge layer was coherently grown at a rate of 1 nm/min at substrate temperature of 400ºC. *In-situ* reflection high energy electron diffraction (RHEED) was used to verify the quality of the surface prior to and during growth. The RHEED patterns for $In_xGa_{1-x}As$ and Ge are 2×4 and 1×2, respectively. Finally, the samples were transferred back into the III-V chamber, where an $In_xGa_{1-x}As$ cap layer was grown to form a Ge QW, eliminate surface states, and improve carrier confinement during optical characterization. For Ge QDs, 4-monolayers (MLs) of Ge (about 5.3 Å) were grown on $In_{0.3}Ga_{0.7}As$ buffer layers at substrate temperatures of 500°C. In-situ RHEED of Ge QDs showed spotty dot pattern, indicating a 3D growth. 20 nm $In_{0.3}Ga_{0.7}As$ cap was grown afterwards for one of the samples. The material qualities were characterized by atomic force microscopy (AFM, Park System XE-70), TEM (Philips CM20 FEG-TEM), XRD (Panalytical

X'Pert Pro), and Raman spectroscopy (Renishaw RM Series System 1000 with a 50 mW Ar^+ laser at 514 nm).

3 Tensile strained Ge QWs

Non-contact mode AFM was used to characterize the sample surface morphology. For Ge QW structures, the root mean square (RMS) surface roughness for a 1 μm× 1 μm region is below 1 nm for various samples. Cross-section TEM was applied to further characterize the crystal quality of tensile-strained Ge between $In_{0.3}Ga_{0.7}As$, as shown in Fig. 1. The interfaces between Ge and InGaAs are smooth and sharp. No threading dislocation in Ge layer is observed in cross section images, which confirms that the defect density is $1\times10^8\ cm^{-2}$ or below. In the high-resolution TEM images, clear lattice fringes confirm the high crystal quality of the Ge layer. The defects and surface roughness in the 10 nm $In_{0.3}Ga_{0.7}As$ cap layer are due to anti-phase domains (APD), which is commonly observed for the polar on non-polar material growths.

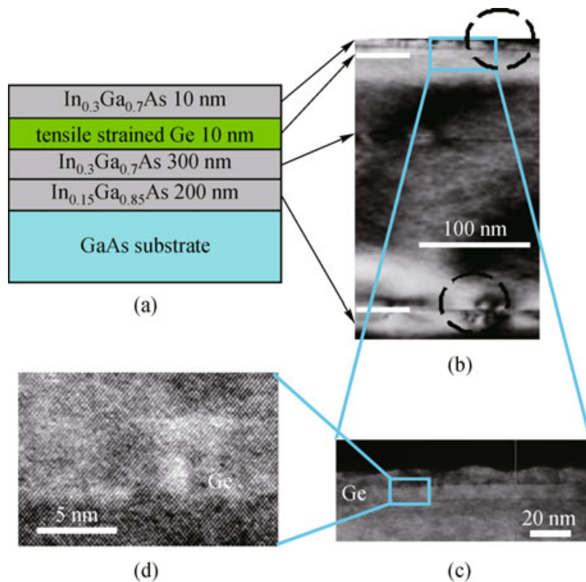

Fig. 1 Cross-section TEM image for strained Ge samples. (a) Schematic of the sample structure; (b) cross-section TEM image of InGaAs buffer layers and the Ge QW; the dash circles are the two selective area diffraction regions in Fig. 2; (c) cross-section TEM image of Ge QW; and (d) high resolution TEM image of Ge QW region

Although the strain in the Ge layer can be calculated from measuring the distance of tens of continuous atom fringes, the results only reflect the local strain and may be affected by non-uniform buffer layer relaxation. However, selected area diffraction (SAD) in TEM can provide strain information from a larger region. Furthermore, the electron beam in SAD TEM is incident parallel to the wafer top surface, thus sampling an effectively thicker region of the QW region than normal XRD. Most importantly, the SAD pattern can be generated from a selected region without background diffraction from the GaAs substrate as well as InGaAs buffer layers. Figure 2 shows the diffraction patterns from two areas, which are indicated by the dashed circles in Fig. 1(b).

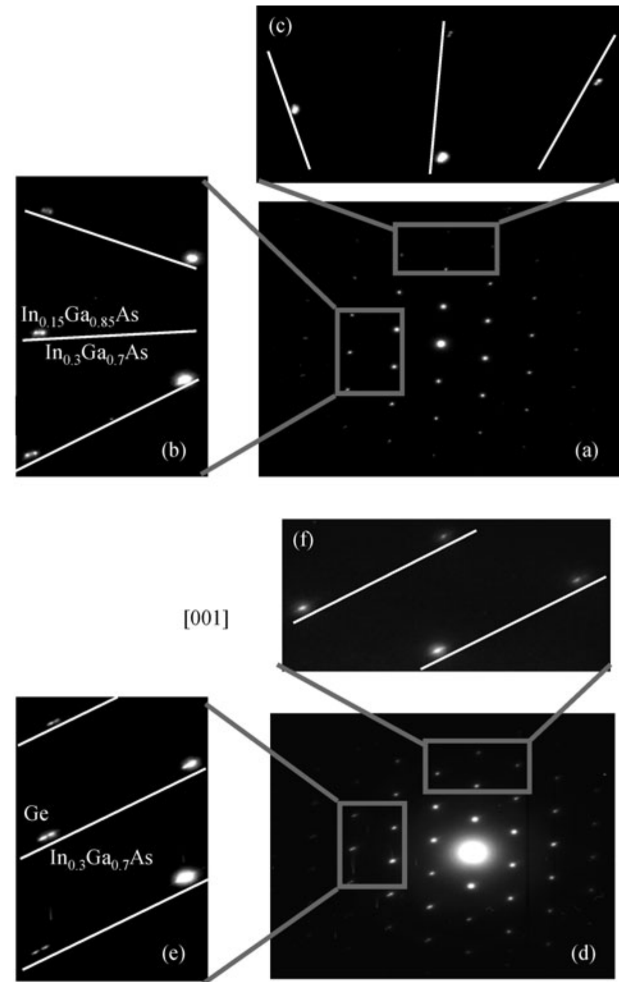

Fig. 2 (a) Selected area diffraction; (b,c) zoom-in images from $In_{0.3}Ga_{0.7}As$ and $In_{0.15}Ga_{0.85}As$ buffer layers; (d) diffraction pattern and (e, f) zoom-in images from $In_{0.3}Ga_{0.7}As$ and Ge layers shown in Fig. 1(b)

In the first case, the selected area is chosen at the interface of the $In_{0.3}Ga_{0.7}As$ and $In_{0.15}Ga_{0.85}As$ buffer layers. As can be observed in Figs. 2(a)–2(c), each diffraction spot actually contains two small diffraction spots from the $In_{0.3}Ga_{0.7}As$ and $In_{0.15}Ga_{0.85}As$ buffer layers. Also, each pair of two small spots is aligned and pointed to the original point of the diffraction pattern. Thus, all the buffer layers are almost fully relaxed reflected by the same out-of-plane and in-plane lattice constant. In the second case, only the $In_{0.3}Ga_{0.7}As$ buffer/cap layers and strained Ge layer are selected. A similar diffraction pattern is obtained as shown in Figs. 2(d)–2(f). However,

in this second case, the two spots are aligned and pointed to the [001] direction which is perpendicular to the sample surface. This shows that the Ge epitaxial layer and $In_{0.3}Ga_{0.7}As$ buffer layer have the same in-plane lattice constant and different out-of-plane lattice constants. Thus, the Ge layer is biaxial tensile strained to the InGaAs buffer layers.

Although the diffraction signal from 10 nm Ge layer is below the noise level in XRD measurement, the strain of Ge layers can be determined by the lattice constants of the InGaAs buffer layers, since the Ge layer is almost totally strained to buffer layers proved in SAD TEM. XRD reciprocal space mapping at (004) and (224) Bragg reflections were measured to determine the composition and strain of $In_xGa_{1-x}As$ buffer layers. The InGaAs buffer layers are partially relaxed with 80% to 90% relaxation rates. Thus, the biaxial tensile strain in Ge is 1.84% for the $In_{0.3}Ga_{0.7}As$ buffer sample.

Raman spectroscopy was also used to determine the strain percentage of the Ge layers. The Raman spectra were taken at room temperature in a (001) backscattering geometry. For this configuration, only the longitudinal optical phonon mode is shown. The Raman peaks around 280 cm^{-1} in the spectra correspond to the $In_xGa_{1-x}As$ buffer layers. The peak around 300 cm^{-1} corresponds to Ge longitudinal optical (LO) phonon mode, and it shifts to lower value as the In concentration in the buffer layers is increased, thus indicating greater tensile strain in the Ge. The amount of tensile strain can be calculated from the Raman shift ($\Delta\omega$) relative to the bulk Ge. The equation can be simplified to $\Delta\omega = b\varepsilon_{\|}$, where $\varepsilon_{\|}$ is the biaxial tensile strain and $b = -(415\pm40)$ cm^{-1}. The amount of tensile strain in the Ge calculated from Raman spectroscopy agrees well with XRD calculation, as shown in Table 1.

The low temperature (5 K) PL spectra of a set of Ge samples with different biaxial tensile strain are plotted in Fig. 3. Due to the long wavelength cut-off of our InGaAs detector, only PL signals with wavelengths shorter than 1600 nm were detected. The PL from InGaAs buffer layers at 5 K is shorter than 1300 nm. Thus, the PL signals detected are generated in the Ge QWs only. At 5 K, a weak PL signal at 1.6 μm was observed, which was from phonon assisted indirect band gap radiative recombination processes. However, no PL signal from 0.3% and 0.9% tensile strained Ge layer was detected due to defects from the relaxation in the buffer layer outweighing the benefits from becoming more direct bandgap. Lastly, a strong PL signal was detected for the highly tensile strained (1.8% and 2.33%) samples. A strong increase on PL intensity from the highly tensile strained Ge was observed upon cooling the sample, which was typical for direct band gap material and was reversed for indirect band gap Ge [8].

The band gap energy is determined by the combination of material, strain, temperature, quantum confinement, optical pump intensity, etc. For Ge, the direct band gap energy is 0.8 eV. For 2% biaxial tensile strained bulk Ge at room temperature, the direct band gap energy is reduced to about 0.5 eV [1,3]. When the temperature changes from 300 to 5 K, the bandgap energy is increased by about 0.09 eV for bulk Ge. Further, quantum confinement, especially in the valence band, raised the band gap energy by about 0.13 eV. Also, the pumping laser power further increased the quasi-Fermi level inside Ge layers. Adding these factors together, the direct band gap transition energy for 2% tensile strained Ge QW at 5 K is around 0.72 eV. The detailed calculations for band gap energy are not discussed due to the inaccuracy of electronic parameters under such high tensile strains, low temperatures and quantum confinements. However, through the rough estimations, the bandgap energy for Ge QWs at 5 K fitted our experimental results. Although it is difficult to give a precise calculation of the band gap energy for highly strained Ge, the dramatic increase of PL intensity with high biaxial tensile strained Ge as well as the dramatic increase of PL at low temperature indicated that direct band gap Ge is achieved under high biaxial tensile strain.

4 Tensile strained Ge QDs

When the growth temperature is increased to 500ºC, the growth mode of Ge is changed from planar growth to three-dimension growth, and self-assembled Ge QDs form. The 1 μm × 1 μm region AFM image of Ge QD on $In_{0.3}Ga_{0.7}As$ buffer without cap is shown in Fig. 4. The dots are circular in shape without obvious facets compared to Ge QD on Si substrate. Randomly choosing 27 dots in the AFM image, the average diameter is calculated as (41.67 ± 4.75) nm, and the height is (4.83 ± 0.65) nm. The density of the dots is about 375 dots/μm^2. SEM picture of the same sample is shown in Fig. 5. The white dots are Ge QDs and their size and shape agree with the AFM

Table 1 Biaxial tensile strain inside Ge with different InGaAs buffer layers as measured by Raman and XRD

indium concentration/%	theoretical Ge strain/%	tensile strain of Ge	
		Raman/%	XRD/%
10	0.64	0.26	0.42
20	1.35	0.91	0.93
30	2.07	1.78	1.84
40	2.79	2.35	2.31

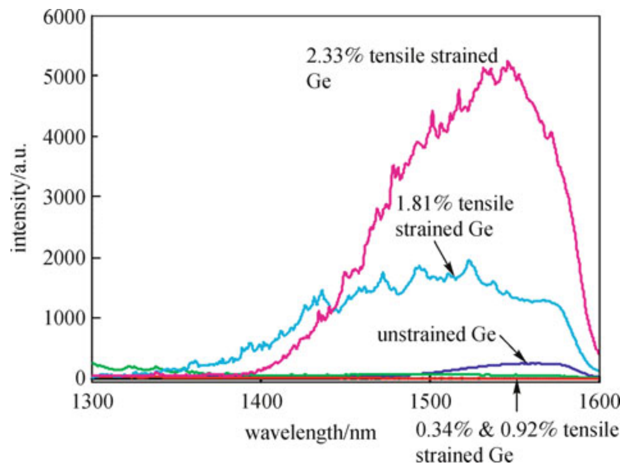

Fig. 3 Low temperature (5 K) PL of different tensile strained Ge layers

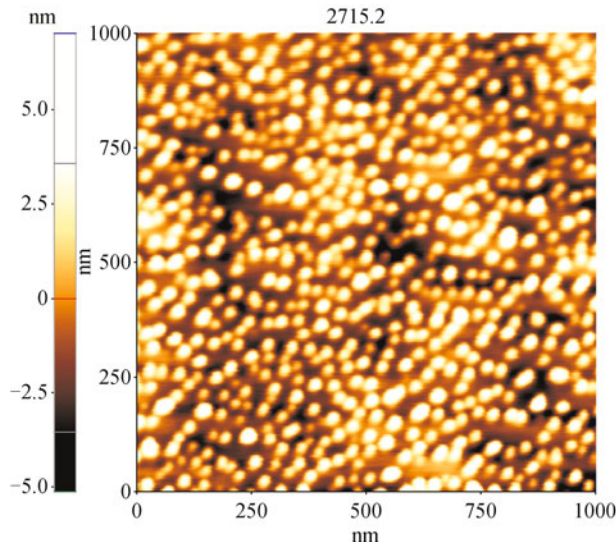

Fig. 4 1 μm × 1 μm AFM image of Ge QDs on InGaAs buffer layer

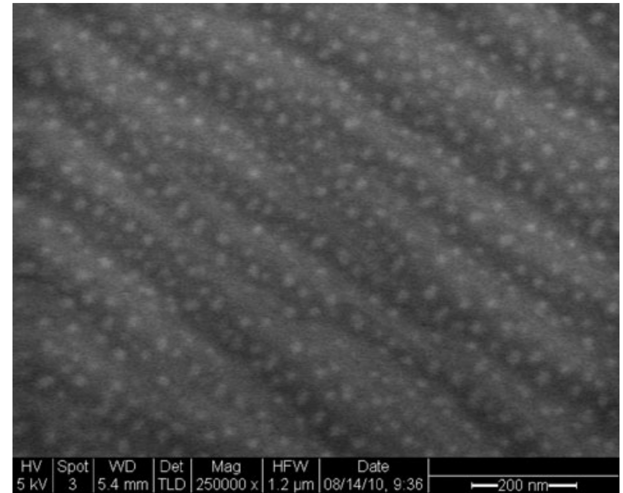

Fig. 5 SEM image of Ge QD on InGaAs buffer layer

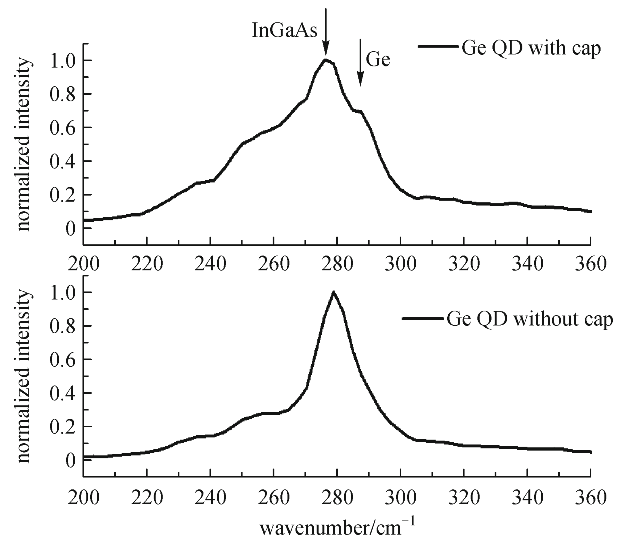

Fig. 6 Raman for Ge QD with and without InGaAs capping layer

measurements. The ripples in the background are due to the surface roughness of InGaAs layers.

Raman spectroscopy was also used to determine the strain percentage of the Ge QD as shown in Fig. 6. Without the InGaAs cap layer, the Ge Raman peak cannot be detected due to the small volume and discontinuity of each dot. However, the Ge QD Raman peak shows up in the sample with InGaAs cap layer. The peak around 280 cm^{-1} in the spectra corresponds to the GaAs-like LO mode from the $In_xGa_{1-x}As$ buffer layer, and the peak around 289 cm^{-1} corresponds to the Ge QDs. The pure Ge Raman peak is at 299.15 cm^{-1} (not shown here), so the strain is calculated to be 2.46% ± 0.2%. The calculation is based on the biaxial strain coefficient, but for buried QDs, the strain status is more complicated than biaxial strain, which causes some discrepancy between the strain of Ge QDs and Ge QWs on the same InGaAs buffers. In summary, at 500°C growth temperature, the Ge growth mode changes to 3D growth and tensile strain Ge QDs are achieved.

5 Conclusions

In summary, we had used MBE to grow up to 2.33% biaxial tensile strained Ge QWs and 2.46% tensile strain Ge QDs on $In_xGa_{1-x}As$ buffer layers, producing the highest reported strain in Ge to the best of our knowledge. Material qualities and strain have been characterized using TEM, AFM, XRD, and Raman spectroscopy. The strains measured in the Ge from different methods are all in very good agreement with each other and match theoretical

predictions. Furthermore, low-temperature PL shows a strong increase in PL intensity with higher strain and lower temperature, which indicates a direct-bandgap tensile-strained Ge has been achieved, and it is a possible candidate for future group-IV laser.

References

1. Fischetti M V, Laux S E. Band structure, deformation potentials, and carrier mobility in strained Si, Ge, and SiGe alloys. Journal of Applied Physics, 1996, 80(4): 2234–2252
2. Bai Y, Lee K E, Cheng C, Lee M L, Fitzgerald E A. Growth of highly tensile-strained Ge on relaxed $In_xGa_{1-x}As$ by metal-organic chemical vapor deposition. Journal of Applied Physics, 2008, 104(8): 084518
3. Liu J, Cannon D D, Wada K, Ishikawa Y, Jongthammanurak S, Danielson D T, Michel J, Kimerling L C. Silicidation-induced band gap shrinkage in Ge epitaxial films on Si. Applied Physics Letters, 2004, 84(5): 660–662
4. Kurdi E M, Bertin H, Martincic E, Kersauson M, Fishman G, Sauvage S, Bosseboeuf A, Boucaud P. Control of direct band gap emission of bulk germanium by mechanical tensile strain. Applied Physics Letters, 2010, 96(4): 041909
5. Takeuchi S, Sakai A, Nakatsuka O, Ogawa M, Zaima S. Tensile strained Ge layers on strain-relaxed $Ge_{1-x}Sn_x$/virtual Ge substrates. Thin Solid Films, 2008, 517(1): 159–162
6. Nataraj L, Xu F, Cloutier S G. Direct-bandgap luminescence at room-temperature from highly-strained germanium nanocrystals. Optics Express, 2010, 18(7): 7085–7091
7. Lin H, Huo Y J, Rong Y W, Chen R, Kamins T I, Harris J S. X-ray diffraction analysis of step-graded $In_xGa_{1-x}As$ buffer layers grown by MBE. Journal of Crystal Growth, 2011, 323(1): 17–20
8. Sun X C, Liu J F, Kimerling L C, Michel J. Direct gap photoluminescence of n-type tensile-strained Ge-on-Si. Applied Physics Letters, 2009, 95(1): 011911